

backs used to obtain the medium restraint levels. The restraint level was qualitatively indicated by the measurements of the inward contraction of four points located on either side of the weld as shown in Fig. 1.

Postweld Test Procedures

Hydrogen Sampling

Individual hydrogen samples were removed by inserting a 7 mm (0.3 in.) I.D. silica pipette into the molten pool during the welding process, and drawing a 100 to 150 mm (3.94 to 5.91 in.) molten sample of the weld. A spring-loaded grease-damped 50 ml syringe acted as the vacuum device to draw and hold the sample in the silica pipette. Once the sample was taken, the silica pipette was broken and crushed in a bucket of water, and the water-quenched sample was removed, washed in alcohol, and placed in a container of dry ice.

The total time for sampling was approximately 15 s for each sample. After all the samples were taken, they were placed in a cooled vice, broken in half, and then transferred to tubes containing mercury, as per ISO 3460 for determining the diffusible hydrogen content (Ref. 9).

From a single weld, four hydrogen samples were taken from three locations: approximately 230, 380, and 530 mm (9.06, 15.0, and 20.9 in.) above the weld start. No samples were taken at the top of the first shoe (50mm—1.96 in.—above the weld start) initially. However, at the later stages of the present study, it was felt that a hydrogen sample taken at the top of the first shoe might produce a sample of higher hydrogen content than from the other locations, as most of the

grain boundary cracks found were situated close to the bottom portion of the weld.

Mechanical Testing

The finished electroslag weld was left in the fixture for 48 h before the weld was sectioned. Weld metal tensile and bend test specimens were machined from T/4 locations of the weld at levels of 90 to 240 mm (3.5 to 9.45 in.) from the top of the weld.

Tensile and bend tests were performed on a Baldwin Universal testing machine according to the ASTM Specification (Ref. 10). The hardness of some welds was measured using a Vickers hardness testing machine with a 10 kg load.

Metallography

One transverse and one longitudinal section were cut out from both the top and bottom of the weld. The sections were next surface ground and dye penetrant checked using Ardrex 985-P2 high sensitivity penetrant with Ardrex 9D6 developer. The cracks were observed using ultraviolet light. The number of cracks and their locations were recorded. These specimens were then etched with 10-15% HNO₃ acid in water to reveal the weld profile.

The specimens containing the cracks were further sectioned in the vicinity of the cracks for microscopic examination. The polished sections were etched with 2% nital to reveal the transformed structure and etched with either Oberhoffer's reagent or Saspa etch (saturated picric acid etch with a wetting reagent—Ref. 11) to reveal the solidification structure.

The specimens were then examined with an optical microscope.

Fractography

Further characterization of the cracks was performed by examining the surfaces of some cracks in a Cambridge scanning electron microscope (SEM). The cracks were generally small and before the surface could be examined the cracks had to be opened. This was accomplished by first reducing the thickness of the specimen and then breaking open the cracks with a hammer blow at low temperature. One-half of the crack was then placed in an inhibited acid solution to remove rust or corrosion products.

The inhibited acid solution does not attack the steel, but removes the inclusions. Therefore, to preserve the inclusions (if any) on the cracked surface, certain specimens containing cracks were not etched or cleaned after opening the crack and before being examined. The inclusions which were seen on the crack surface were analyzed qualitatively using a KeveXray x-ray energy analyzer attached to the SEM.

Results

Diffusible Hydrogen Content of the Electroslag Weld

The average room temperature diffusible hydrogen content of the electroslag weld metal (hereafter referred to as weld metal hydrogen content) for all the welds in Parts 1 and 2 of the study is shown in Tables 3 and 4. The values for the average weld metal hydrogen content given in Table 4 are calculated from the results of samples extracted from the three locations mentioned earlier and the individual weld metal hydrogen values for some of the electroslag welds are shown in Table 5.

The electroslag welds performed with the soaking wet flux, the high restraint, and the high humidity atmosphere had a sample extracted from the top of the first shoe, as well as the three standard locations. The effect of the additional sample location on the average weld metal hydrogen content is given in Table 4. Plots of the hydrogen distribution for some of the welds performed in Part 2 of the present study are shown in Fig. 3.

The total and the diffusible hydrogen content of the samples extracted from an electroslag weld performed using the standard conditions is shown in Table 6. The difference between the total and the diffusible hydrogen is within the precision of the diffusible hydrogen measurements. The total hydrogen content of the wire used to deposit the electroslag welds in Part 1 and 2 of this work was between 0.1 and 0.3 ml/100 g, as measured by the subfusion vacuum extraction technique.

Table 3—Diffusible Hydrogen Content of Electroslag Weld Metal—Part 1

Weld no.	Flux type	Flux condition	Atmosphere condition	Slag cap height mm	Average weld metal hydrogen content, ml/100g
1	Arcos BV	Wet	Humid	64	2.1
2	"	Dry	Dry	64	1.9
3	"	Dry	Dry	45	1.0
4	"	Wet	Humid	51	1.3
5	"	Wet	Humid	51	2.0
6	"	Wet	Dry	51	1.2
7	"	Very wet	Dry	51	1.3
8	"	Very wet	Humid	32	2.0
9	"	Dry	Humid	45	2.2
10	"	Very wet	Humid	48	1.2
11	Hobart PF201	Dry	Dry	30	1.5
12	"	Wet	Dry	35	0.7
13	"	Dry	Humid	45	1.3
14	"	Very wet	Dry	45	0.9
15	"	Wet	Humid	35	0.9
16	"	Very wet	Humid	38	0.8
17	Linde 124	Dry	Dry	45	1.0
18	"	Very wet	Humid	51	1.3
19	"	Very wet	Dry	51	1.1
20	"	Dry	Humid	51	1.5

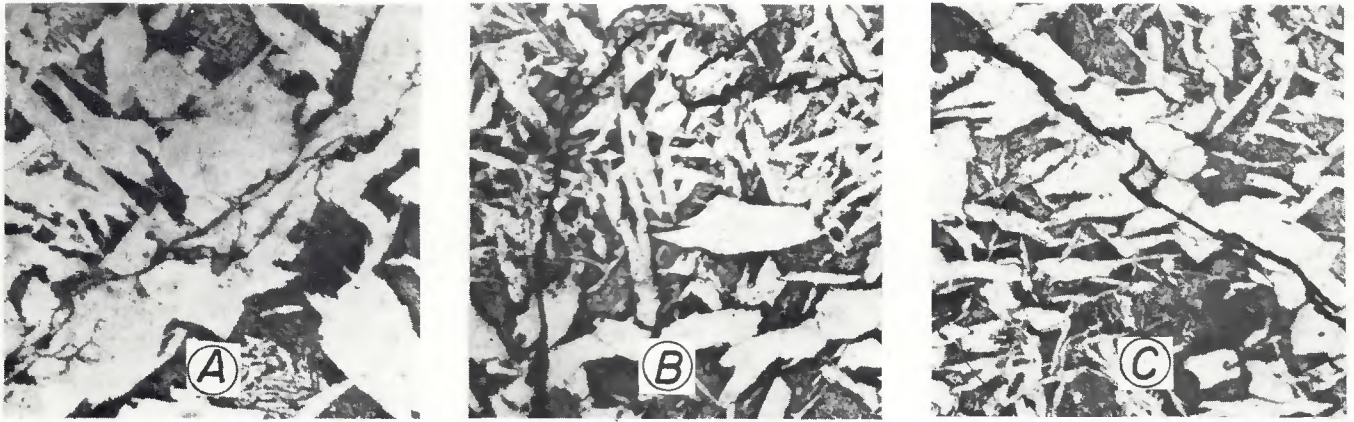


Fig. 6—Intergranular cracks and the cross sections of the electroslag welds showing: A—inclusions at the crack (ESW 44), X800; B and C—sheared ferrite grains and the termination of cracks away from the grain boundary (ESW 30), X500 (A, B and C reduced 28% on reproduction)

welds made by electroslag processes using a shielding of saturated water vapor. Such accumulations of hydrogen were not observed in the present study at any humidity levels of atmosphere.

Zeke, *et al.* (Ref. 14) explained that hydrogen may accumulate, decrease, or remain constant as the length of the cast ingots increases and the exact hydrogen distribution is related to the filler metal/flux combination used in the electroslag process. The choice of flux had no effect on the distribution of hydrogen in the electroslag welds in the present study.

Hydrogen Levels

The evidence gathered in Part 1 suggests that hydrogen pickup in weld metal is virtually the same with either Hobart PF201 or Linde 124 flux; the basicity of both being approximately 1. A slightly larger hydrogen content is evident when Arcos BV flux with basicity 3 is used.

This result is in agreement with that of Nakano, *et al.* (Ref. 5) who report that higher flux basicity increases the hydrogen content in the slag and in the weld metal, and that the diffusible hydrogen levels are mainly controlled by the distribution of hydrogen between slag and metal. However, the degree to which the amount of hydrogen is affected by flux basicity is not comparable since an increase in flux basicity, from 0.42 to 1.33 in Nakano's study, resulted in a substantial increase in hydrogen from 3 ml/100 g to 8 ml/100 g. On the other hand, when the basicity of the flux is increased in the present work from 1 to 3, only a slight increase in hydrogen results, 1 ml/100 g to 2 ml/100 g.

The presence of humid atmosphere or the moisture content of the wet or very wet flux does not result in a significant gain in hydrogen content in the weld metal for any of the three fluxes. This may be due to the small moisture content of the flux or the air.

Part 2 of the present work indicates that hydrogen content in the electroslag

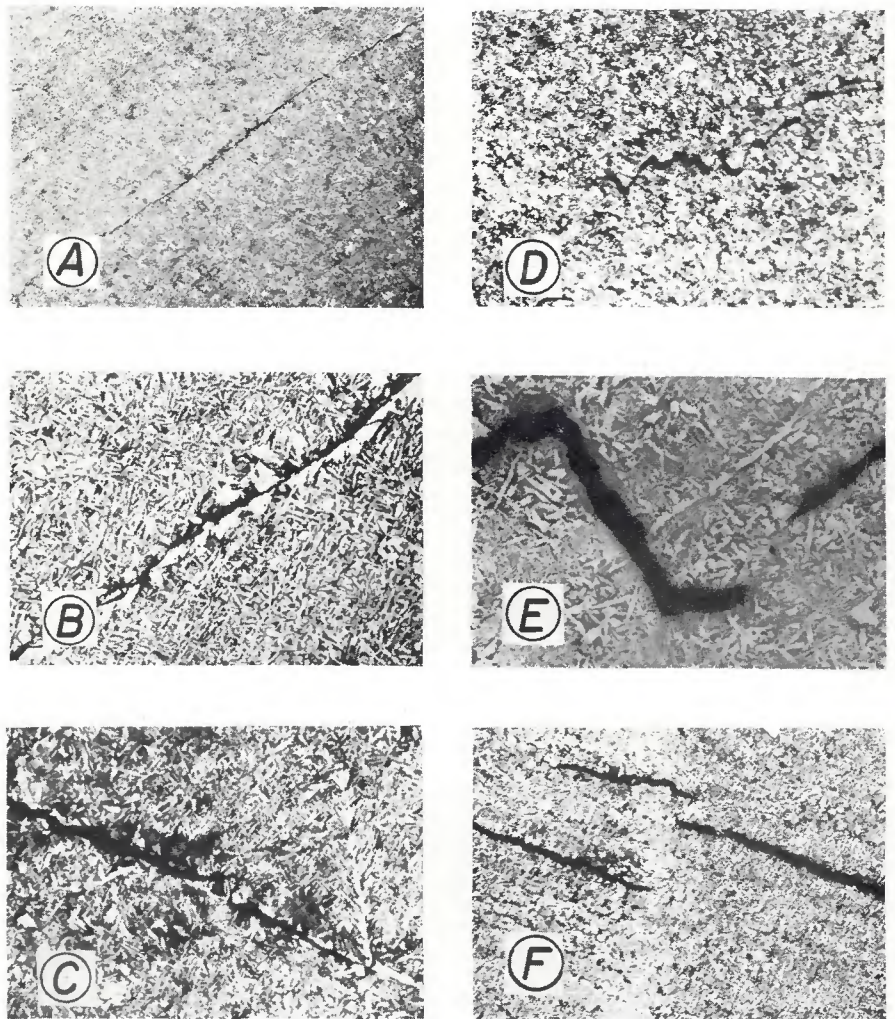


Fig. 7—Solidification structures around cracks, X25 (reduced 28% on reproduction): A—transverse section (ESW 30) intergranular crack, Saspas etch; B—longitudinal section (ESW 30) intergranular crack, Saspas etch; C and D—same as A and B but with Oberhoffer's etch; E—transverse section (ESW 31) transgranular crack, Saspas etch; F—longitudinal section (ESW 33) transgranular crack

